PHYSICAL REVIEW B **95**, 121401(R) (2017)

Path-dependent initialization of a single quantum dot exciton spin in a nanophotonic waveguide

R. J. Coles,[1] D. M. Price,[1] B. Royall,[1] E. Clarke,[2] M. S. Skolnick,[1] A. M. Fox,[1,*] and M. N. Makhonin[1,†]

[1]*Department of Physics and Astronomy, University of Sheffield, Sheffield S3 7RH, United Kingdom*

[2]*Department of Electronic and Electrical Engineering, EPSRC National Centre for III-V Technologies, University of Sheffield, Sheffield S1 3JD, United Kingdom*

(Received 6 September 2016; published 6 March 2017)

We demonstrate a scheme for in-plane initialization of a single exciton spin in an InGaAs quantum dot (QD) coupled to a GaAs nanobeam waveguide. The chiral coupling of the QD and the optical mode of the nanobeam enables spin initialization fidelity approaching unity in magnetic field $B = 1$ T and > 0.9 without the field. We further show that this in-plane excitation scheme is independent of the incident excitation laser polarization and depends solely on the excitation direction. This scheme provides a robust in-plane spin excitation basis for a photon-mediated spin network for quantum information applications.

DOI: 10.1103/PhysRevB.95.121401

The spin states of quantum dots (QDs) have been recognized as promising solid-state qubits for applications in quantum information processing, with a number of key operations having already being demonstrated using off-chip excitation schemes [1,2]. However, the development of scalable and compact spin networks [3,4] based on QDs requires that the dots should be embedded on-chip within photonic structures. This has the added benefit of enhancing the light-matter interaction and providing an efficient mechanism for the generation and manipulation of single photons on-chip [5]. The establishment of spin networks then relies on demonstrating faithful communication of spin information between matter qubits (QD spins) via flying qubits (photons) within a photonic circuit [6,7]. To this end, an efficient on-chip spin-photon interface is required to map the spin of the matter qubit onto the spin or direction of the flying qubit.

Directional emission is an example of optical spin-orbit coupling and is a general property of wavelength-scale optical systems due to the existence of elliptically polarized electric fields in guided modes [8,9]. Such unidirectional phenomena have been observed in a variety of physical systems using several different types of nanophotonic structures [10–19]. These experiments demonstrate spin-to-path conversion where the emitter spin is directly mapped to the propagation direction in the photonic structure. However, for on-chip communication using spins, photon path to spin initialization, or flying to static qubit conversion, is essential. Such reversibility has been demonstrated in a passive silicon photonic device consisting of a microdisk coupled to a waveguide [17] and for a single ^{85}Rb atom evanescently coupled to a whispering gallery mode resonator [11]. However, path-to-spin initialization of a solid-state quantum emitter in a scalable architecture remains to be demonstrated. Realization of this goal further expands the field of chiral quantum optics, enabling the realization of nonreciprocal single-photon devices, deterministic spin-photon interfaces, spin-spin transfer, and on-chip quantum logic in integrated quantum-optical circuits [9]. In addition, since these principles hold for many nanophotonic systems, applications of this approach may extend beyond quantum-optical devices to provide novel experimental approaches for research topics including spin-Hall phenomena, spin-controlled light shaping, and novel designs of optical sensors [8,16].

In this Rapid Communication we demonstrate path-to-spin initialization of a single QD exciton spin in a single-mode nanobeam waveguide using spin-to-path readout to measure the fidelity of the initialization process. We show that a photon propagating in a specific direction excites a correspondingly polarized exciton spin state when absorbed by the QD. This direction-dependent initialization of a single QD exciton spin is a key goal towards the realization of a quantum spin network, enabling photon mediated spin-to-spin communication on-chip. Furthermore single photons are emitted in a direction that may be controlled by coherent manipulation of the spin state of the exciton, which opens avenues towards on-chip quantum logic.

Our scheme for QD exciton spin initialization is presented in Fig. 1(a), which is based on the chiral coupling of the QD to the waveguide mode. If a QD is located or deterministically placed at a chiral point, where the electric field is circular (denoted C point), the exciton spins will couple to circularly polarized photons which propagate in opposite directions along the waveguide with fidelity $\sim$1 [10]. The consequence is that a single spin eigenstate of the QD exciton can be addressed by controlling the propagation direction of the incident photon. The direction of the incident photon is controlled by selectively applying laser light to one end of the waveguide. Upon recombination of the exciton, in the absence of spin manipulation or scattering, the emitted photon propagates only in the same direction as the incident photon. The fidelity of spin initialization can therefore be characterized by comparison of the photoluminescence (PL) intensity from each end of the waveguide.

The waveguide device consists of a vacuum-clad single-mode GaAs nanobeam waveguide containing InGaAs QDs in the xy plane at $z = 0$. Grating couplers [20] are added to each end, as shown in the scanning electron microscope image of Fig. 1(b), to allow free space coupling to the waveguide mode [10,19,21–24]. The waveguide possesses quasicontinuous translational symmetry, so the constraints on the emitter location along x are relaxed relative to devices based upon photonic crystal waveguides [19,25]. This allows for a higher probability of chirally-coupled QDs when randomly grown

*mark.fox@sheffield.ac.uk
†m.makhonin@sheffield.ac.uk

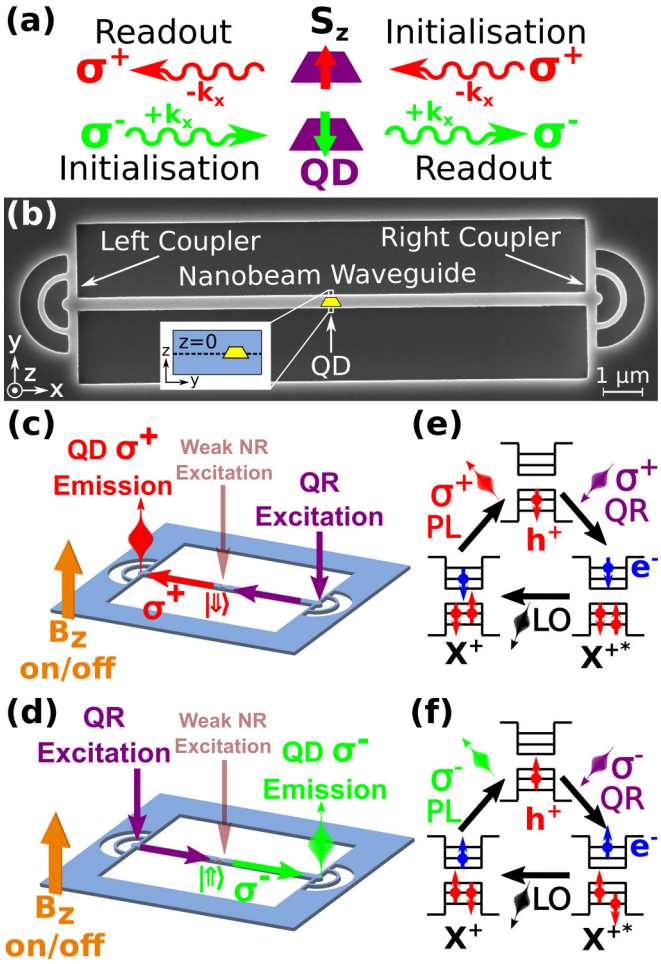

FIG. 1. (a) Schematic illustrating the relationship between photon polarization (σ^+,σ^-), propagation direction ($-k_x$, $+k_x$), and trion pseudospin ($\uparrow$, $\downarrow$) for optical readout and initialization of a quantum dot spin at a chiral point. (b) Scanning electron microscope image of the device. (inset) Schematic cross section of the waveguide. (c) and (d) Schematic of the experimental arrangement for QD exciton spin initialization from the (c) right and (d) left coupler. The QD is located at a chiral point in the waveguide. (e) and (f) Schematics showing the excitonic species involved in quasiresonant (QR) excitation of the X^+ transition for (e) σ^+ (f) σ^--polarized excitation and emission. The longitudinal optic phonon is denoted as LO.

and a larger tolerance in the position for deterministically positioned QDs, as shown in Ref. [10]. The sample is held at 4 K in a liquid helium bath cryostat, and a magnetic field B_z can be applied normal to the device plane. A confocal microscopy system with two motorized scanning mirrors allows spatially resolved excitation and separate detection of photoluminescence (PL) in the sample. For further details on the experimental setup see the Supplemental Material in Ref. [24].

In order to demonstrate path-dependent spin initialization, a single QD that exhibits a high degree of spin-path conversion (spin readout) was first selected using the same methods presented in Ref. [10]. In the Supplemental Material in Ref. [24] we present identification of a QD which resides very close to a C point and show that X^+ trion recombination within this QD exhibits a high degree of spin to path conversion. The observation of high contrast unidirectional emission shows that photons originating from different spin states of the exciton propagate in opposite directions in the waveguide mode. Here we show that a photon propagating in a given direction in the waveguide will excite only one of the two exciton spin eigenstates upon absorption by the QD. This same QD is used for subsequent demonstrations of spin initialization in this paper.

The use of a charged exciton is ideal for a spin-photon interface as selection rules dictate that the polarization of emitted photons is always circular. This eliminates the effects of fine structure splitting, as found for the neutral exciton X^0, and facilitates direct mapping of the exciton spin to the helicity of photon polarization. Resonant excitation of the X^+ trion would enable coherent initialization and control of the residual hole spin [26–29]. However, distinction between photons emitted by the QD and from a resonant laser in a waveguide geometry is nontrivial [22]. We note that quasiresonant (QR) p-shell excitation of the QD exciton has been shown to preserve the spin of the incident photon and to initialize the s-shell exciton spin eigenstates with fidelity of >0.95 in planar samples [30], while allowing for effective spectral filtering of QD PL emission. Therefore we employ a tunable diode laser coupled to the p-shell resonance of the X^+ trion via the grating coupler (identification of the p-shell resonance is presented in the Supplemental Material in Ref. [24]). As shown schematically in Figs. 1(c) and 1(d) QR laser photons are scattered from the coupler along the waveguide towards the QD at a C point, where the photon spin is transferred to the spin state of the p-shell X^+ trion on absorption (explained in more detail later). An LO phonon assisted process allows the carriers to relax rapidly to the ground state in a spin conserving process. Recombination of the s-shell X^+ trion then produces a σ^+/σ^- polarized photon which propagates either to the left or right coupler depending on the initial spin state. Schematics illustrating the initialization, relaxation, and emission processes are presented in Figs. 1(e) and 1(f). PL emission from the QD is only observed under QR excitation when weak, above band-gap, nonresonant (NR) excitation is also applied which populates the residual charge within the QD (e.g., as in Ref. [22]). This weak NR excitation is applied from directly above the QD in the waveguide as shown in Figs. 1(c) and 1(d).

Figure 2(a) presents exciton PL emission spectra measured from the left coupler for QR excitation on either coupler with $B_z = 1$ T. The magnetic field lifts the degeneracy of the spin eigenstates of the QD exciton through the Zeeman effect and facilitates their identification via emission of circularly polarized photons of different wavelength. When QR excitation is applied to the right coupler, intense PL emission from the σ^+ emission peak is seen. Conversely, for detection on the right coupler, the σ^- peak is most intense when QR excitation is applied to the left coupler, as shown in Fig. 2(b). In both cases only very weak signal is observed with excitation and detection on the same coupler, due to the weak PL emission from the NR laser. These results demonstrate the initialization of the exciton spin using path-spin conversion and subsequent directional re-emission, which can be understood as follows. When QR excitation is applied to the right coupler, the waveguide mode propagating from right to left is excited. Weak NR excitation

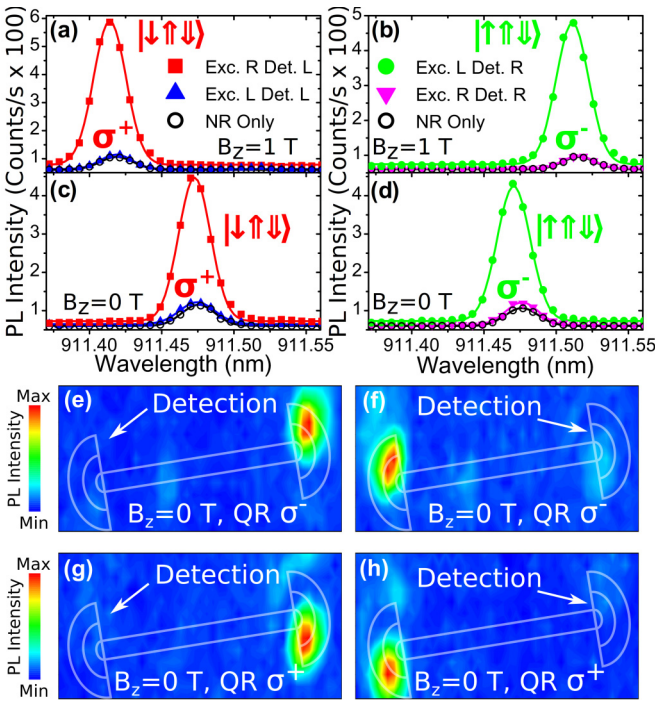

FIG. 2. (a), (b) PL spectra obtained at $B_z = 1$ T when quasiresonantly exciting the QD from each grating coupler with detection fixed at the (a) left and (b) right coupler. (c), (d) PL spectra as in (a), (b) but with $B_z = 0$ T. The legends in (a) and (b) refer to the couplers on which the QR excitation laser and PL detection were located, respectively (L=left coupler, R=right coupler). Spectral data are shown as solid and hollow symbols, with Gaussian fits as solid lines. Spectra with only the weak NR laser applied are shown as hollow circles. (e), (f) Excitation maps obtained by performing a raster scan of the σ^- polarized QR laser over the device while keeping detection fixed at the (e) left and (f) right coupler. (g), (h) Excitation maps as in (e), (f) but with σ^+ laser polarization. All maps recorded PL emission filtered at the QD wavelength at $B_z = 0$ T, and a schematic outline of the waveguide and couplers are overlaid. The apparent rotation of the device from horizontal is due to a small rotation induced by the detection optics.

of the QD located at a C point creates a resident hole with random spin. If this hole is in the $|\Downarrow\rangle$ state, the QD absorbs a σ^+ polarized QR photon from the left propagating waveguide mode which creates an X^+ trion with spin state $|\downarrow\Uparrow\Downarrow\rangle$. This exciton then recombines and emits a σ^+ photon into the same waveguide direction leaving a residual hole state $|\Downarrow\rangle$. The photon is detected from the left coupler as illustrated in Fig. 1(c). If the hole is initially in the $|\Uparrow\rangle$ state, the photon is not absorbed by the QD. When QR excitation is moved to the left coupler, the exciton is prepared in the $|\uparrow\Uparrow\Downarrow\rangle$ spin state and the emitted σ^- photon propagates to the right coupler, as illustrated in Fig. 1(d), leaving a residual hole state $|\Uparrow\rangle$. In the absence of exciton spin flips within the QD, emitted photons from the same coupler where the excitation is applied are not expected, exactly as observed. Directional emission following initialization therefore demonstrates a high degree of spin memory within the QD. Hence the device exhibits path-spin and spin-path conversion $|L\rangle \leftrightarrow |\downarrow\Uparrow\Downarrow\rangle$ and $|R\rangle \leftrightarrow |\uparrow\Uparrow\Downarrow\rangle$ where L and R are the propagation directions of the photon.

To quantify the fidelity of spin initialization, we define the initialization contrast for detection on each grating coupler as

$$C^{\text{init}}_{\text{det.l/r}} = \frac{I_L - I_R}{I_L + I_R}, \tag{1}$$

where the upper case subscripts L/R refer to excitation on either the left or right coupler, the lower case subscripts l/r refer to detection on either the left or right coupler, and $I_{L/R} = I^{\sigma+}_{L/R} + I^{\sigma-}_{L/R}$ where $\sigma^{+/-}$ refer to the PL emission peaks in Figs. 2(a)–2(d). The integrated intensity over each spectral peak where the weak background PL signal due to the NR laser, i_{NR}, is subtracted from the PL signal with both lasers, i_{QR}, as $I = \int (i_{QR} - i_{NR}) d\lambda$, is used to calculate the initialization contrast. We extract $C^{\text{init.}}_{\text{det.l}} = -0.96 \pm 0.05$ and $C^{\text{init.}}_{\text{det.r}} = 0.99 \pm 0.06$ for this QD. The small difference in initialization contrasts is attributed to dissimilar, weak reflections from the grating couplers due to fabrication imperfections. The need for subtraction is not a fundamental limitation of the system but is due to the use of a NR laser to populate the additional hole for X^+. We note that p-type doping of the sample can completely eliminate the need for an NR laser [31] and thus make PL subtraction redundant. Autocorrelation measurements are presented in the Supplemental Material in Ref. [24] for the PL emission lines in Figs. 2(a)–2(d) which confirm that the single photon emission character is retained under QR excitation.

Very high initialization and readout contrasts highlight the practicality of the device as a spin-photon interface. When one considers the application of the device, however, the requirement for an external magnetic field may present an obstacle to scalability under some circumstances. We therefore repeated the experiments for $B_z = 0$ T and the resulting spectra are presented in Figs. 2(c) and 2(d). Large initialization contrasts in the absence of magnetic field are still observed with $C^{\text{init.}}_{\text{det.l}} = -0.96 \pm 0.03$ and $C^{\text{init.}}_{\text{det.r}} = 0.92 \pm 0.03$. These slightly reduced contrast values are attributed to electron dephasing caused by the Overhauser field of nuclei in the QD at $B_z = 0$ T [31,32].

To demonstrate that the initialized spin is determined by the direction of excitation only and not the incident QR laser polarization, we provide excitation maps for different QR laser polarizations. The maps are obtained using a raster scan of QR excitation over the device while keeping the detection fixed at one grating coupler, filtered at the QD emission wavelength, and without an applied magnetic field. The results of these measurements are presented in Figs. 2(e) and 2(f) for detection on the left and right couplers, respectively, using σ^- polarized excitation, while in Figs. 2(g) and 2(h) a σ^+ polarized laser is used. As can be clearly seen from these data, intense PL emission from the QD is observed only when exciting and detecting from opposite couplers; the initialization does not depend on the laser polarization. Since the chiral coupling of the QD and the waveguide mode is determined by the local electric field polarization of the waveguide mode, the initialization contrast is expected to be independent of the QR polarization. The polarization of the incident laser only determines the overlap with the free space optical modes of the grating coupler and hence the efficiency with which the waveguide mode is excited. The independence of the waveguide mode on the incident laser polarization is discussed in more detail in the Supplemental Material in Ref. [24].

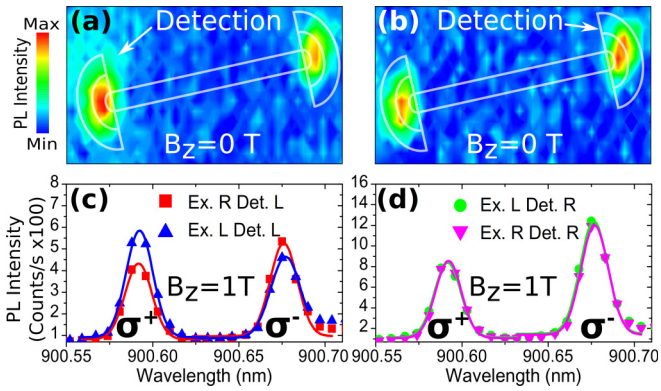

FIG. 3. (a), (b) Excitation maps obtained by a raster scan of QR excitation over a device containing a nonchirally coupled QD while keeping detection fixed at the (a) left and (b) right grating couplers at $B_z = 0$ T. All maps recorded PL emission filtered at the QD wavelength and a schematic outline of the waveguide and couplers is overlaid. As in Fig. 2, the apparent rotation of the device from horizontal is due to a small rotation induced by the detection optics. (c), (d) Corresponding PL spectra obtained when exciting the QD from each coupler with detection fixed at the (c) left and (d) right coupler when an external magnetic field of $B_z = 1$ T is applied. Spectral data are shown as solid symbols, with an experimental Gaussian fit to the data shown as a solid line.

To verify that the high degree of spin initialization arises from the chiral coupling of the QD with the waveguide mode, measurements were also made on a QD which does not exhibit unidirectional emission. For this to occur the QD must be located close to the center of the waveguide, where the modal fields are linear (termed L points). The QD that is symmetrically coupled is identified from NR excitation measurements first with the main difference that both σ^+/σ^- are detected with approximately equal intensity from both couplers. The results of the QR excitation experiments on this nonchiral QD are presented in Fig. 3. The excitation maps in Figs. 3(a) and 3(b) show almost equal emission intensities when the QD is excited from either grating coupler, independent of which coupler the emission is detected from. These findings are reflected in the measured spectra of Figs. 3(c) and 3(d), where extracted initialization contrasts very close to zero are found with $C^{\text{init.}}_{\text{det.l}} = (9 \pm 1)\times 10^{-3}$ and $C^{\text{init.}}_{\text{det.r}} = (-13 \pm 1)\times 10^{-3}$. These results are strikingly different to those for the QD at a C point in Fig. 2 where a clear asymmetry is seen in PL intensity between the grating couplers. These data confirm that the high fidelity of spin-path conversion for the displaced QD is indeed due to chiral coupling between the exciton emission and the waveguide mode.

To conclude, we demonstrate in-plane initialization and readout of a charged exciton spin in a QD chirally coupled (located at a C point) to a single mode waveguide using a quasiresonant excitation scheme. Spin initialization is demonstrated with high directionality contrasts $\sim$1 at $B_z = 1$ T and $>$0.9 at $B_z = 0$ T. We compare with a nonchirally coupled QD (located at an L point) and show that the high fidelity of spin preparation is indeed due to the chiral coupling of the QD. Furthermore, we show that the addressing of each exciton spin state is determined by the excitation path and is independent of the incident laser polarization. The findings and techniques presented establish a method for communication between two or more quantum dots on-chip and have the potential to contribute to the creation of spin-optical on-chip networks [9]. Furthermore, the scheme demonstrated here is applicable to on-chip spin logic operating at ultrafast speeds, chip scale optical isolators, and the investigation of a diversity of spin-orbit coupling phenomena in a variety of classical and quantum systems [8,16].

The authors gratefully acknowledge funding from EPSRC under research Grant Nos. EP/J007544/1 and EP/N031776/1. Data supporting this study are openly available from the University of Sheffield repository, see Ref. [33].

[1] R. J. Warburton, Nat. Mater. **12**, 483 (2013).
[2] A. Delteil, Z. Sun, W.-b. Gao, E. Togan, S. Faelt, and A. Imamoglu, Nat. Phys. **12**, 218 (2015).
[3] T. Ramos, B. Vermersch, P. Hauke, H. Pichler, and P. Zoller, Phys. Rev. A **93**, 062104 (2016).
[4] B. Vermersch, T. Ramos, P. Hauke, and P. Zoller, Phys. Rev. A **93**, 063830 (2016).
[5] P. Lodahl, S. Mahmoodian, and S. Stobbe, Rev. Mod. Phys. **87**, 347 (2015).
[6] D. P. DiVincenzo, Fortschr. Phys. **48**, 771 (2000).
[7] S. D. Barrett and P. Kok, Phys. Rev. A **71**, 060310 (2005).
[8] K. Bliokh, F. Rodríguez-Fortuño, F. Nori, and A. Zayats, Nat. Photon. **9**, 796 (2015).
[9] P. Lodahl, S. Mahmoodian, S. Stobbe, P. Schneeweiss, J. Volz, A. Rauschenbeutel, H. Pichler, and P. Zoller, Nature **541**, 473 (2017).
[10] R. J. Coles, D. M. Price, J. E. Dixon, B. Royall, E. Clarke, P. Kok, M. S. Skolnick, A. M. Fox, and M. N. Makhonin, Nat. Commun. **7**, 11183 (2016).
[11] C. Junge, D. O'Shea, J. Volz, and A. Rauschenbeutel, Phys. Rev. Lett. **110**, 213604 (2013).
[12] B. le Feber, N. Rotenberg, and L. Kuipers, Nat. Commun. **6**, 6695 (2015).
[13] I. J. Luxmoore, N. A. Wasley, A. J. Ramsay, A. C. T. Thijssen, R. Oulton, M. Hugues, S. Kasture, V. G. Achanta, A. M. Fox, and M. S. Skolnick, Phys. Rev. Lett. **110**, 037402 (2013).
[14] I. J. Luxmoore, N. A. Wasley, A. J. Ramsay, A. C. T. Thijssen, R. Oulton, M. Hugues, A. M. Fox, and M. S. Skolnick, Appl. Phys. Lett. **103**, 241102 (2013).
[15] R. Mitsch, C. Sayrin, B. Albrecht, P. Schneeweiss, and A. Rauschenbeutel, Nat. Commun. **5**, 5713 (2014).
[16] J. Petersen, J. Volz, and A. Rauschenbeutel, Science **346**, 67 (2014).
[17] F. J. Rodríguez-Fortuño, I. Barber-Sanz, D. Puerto, A. Griol, and A. Martínez, ACS Photon. **1**, 762 (2014).
[18] F. J. Rodríguez-Fortuño, G. Marino, P. Ginzburg, D. O'Connor, A. Martínez, G. A. Wurtz, and A. V. Zayats, Science **340**, 328 (2013).

[19] I. Söllner, S. Mahmoodian, S. L. Hansen, L. Midolo, A. Javadi, G. Kiršansk, T. Pregnolato, H. El-Ella, E. H. Lee, J. D. Song, S. Stobbe, and P. Lodahl, Nat. Nanotechnol. **10**, 775 (2015).

[20] A. Faraon, I. Fushman, D. Englund, N. Stoltz, P. Petroff, and J. Vuckovic, Opt. Express **16**, 12154 (2008).

[21] M. Arcari, I. Söllner, A. Javadi, S. Lindskov Hansen, S. Mahmoodian, J. Liu, H. Thyrrestrup, E. H. Lee, J. D. Song, S. Stobbe, and P. Lodahl, Phys. Rev. Lett. **113**, 093603 (2014).

[22] M. N. Makhonin, J. E. Dixon, R. J. Coles, B. Royall, I. J. Luxmoore, E. Clarke, M. Hugues, M. S. Skolnick, and A. M. Fox, Nano Lett. **14**, 6997 (2014).

[23] N. Prtljaga, R. J. Coles, J. O'Hara, B. Royall, E. Clarke, A. M. Fox, and M. S. Skolnick, Appl. Phys. Lett. **104**, 231107 (2014).

[24] See Supplemental Material at http://link.aps.org/supplemental/10.1103/PhysRevB.95.121401 for further details of sample fabrication, experimental techniques, and supporting experimental and theoretical data.

[25] A. B. Young, A. C. T. Thijssen, D. M. Beggs, P. Androvitsaneas, L. Kuipers, J. G. Rarity, S. Hughes, and R. Oulton, Phys. Rev. Lett. **115**, 153901 (2015).

[26] M. Kroner, A. O. Govorov, S. Remi, B. Biedermann, S. Seidl, A. Badolato, P. M. Petroff, W. Zhang, R. Barbour, B. D. Gerardot, R. J. Warburton, and K. Karrai, Nature (London) **451**, 1022 (2008).

[27] T. M. Godden, J. H. Quilter, A. J. Ramsay, Y. Wu, P. Brereton, S. J. Boyle, I. J. Luxmoore, J. Puebla-Nunez, A. M. Fox, and M. S. Skolnick, Phys. Rev. Lett. **108**, 017402 (2012).

[28] K. De Greve, P. L. McMahon, D. Press, T. D. Ladd, D. Bisping, C. Schneider, M. Kamp, L. Worschech, S. Hoefling, A. Forchel, and Y. Yamamoto, Nat. Phys. **7**, 872 (2011).

[29] A. J. Brash, L. M. P. P. Martins, F. Liu, J. H. Quilter, A. J. Ramsay, M. S. Skolnick, and A. M. Fox, Phys. Rev. B **92**, 121301 (2015).

[30] A. Boyer de la Giroday, A. J. Bennett, M. A. Pooley, R. M. Stevenson, N. Skold, R. B. Patel, I. Farrer, D. A. Ritchie, and A. J. Shields, Phys. Rev. B **82**, 241301 (2010).

[31] Y. Cao, A. J. Bennett, I. Farrer, D. A. Ritchie, and A. J. Shields, Phys. Rev. B **92**, 081302 (2015).

[32] E. A. Chekhovich, M. N. Makhonin, A. I. Tartakovskii, A. Yacoby, H. Bluhm, K. C. Nowack, and L. M. K. Vandersypen, Nat. Mater. **12**, 494 (2013).

[33] http://dx.doi.org/10.15131/shef.data.4633522.